



Contents lists available at ScienceDirect

## Bioorganic &amp; Medicinal Chemistry Letters

journal homepage: [www.elsevier.com/locate/bmcl](http://www.elsevier.com/locate/bmcl)

## Pyridyl-pyrimidine benzimidazole derivatives as potent, selective, and orally bioavailable inhibitors of Tie-2 kinase

Victor J. Cee<sup>a,\*</sup>, Alan C. Cheng<sup>b,f</sup>, Karina Romero<sup>a</sup>, Steve Bellon<sup>b,f</sup>, Christopher Mohr<sup>b,f</sup>, Douglas A. Whittington<sup>b,f</sup>, Annette Bak<sup>c</sup>, James Bready<sup>e</sup>, Sean Caenepeel<sup>e</sup>, Angela Coxon<sup>e</sup>, Holly L. Deak<sup>a</sup>, Jenne Fretland<sup>d,g</sup>, Yan Gu<sup>b,f</sup>, Brian L. Hodous<sup>a</sup>, Xin Huang<sup>b,f</sup>, Joseph L. Kim<sup>b,f</sup>, Jasmine Lin<sup>d,g</sup>, Alexander M. Long<sup>b,f</sup>, Hanh Nguyen<sup>a</sup>, Philip R. Olivieri<sup>a</sup>, Vinod F. Patel<sup>a</sup>, Ling Wang<sup>e</sup>, Yihong Zhou<sup>d,g</sup>, Paul Hughes<sup>e</sup>, Stephanie Geuns-Meyer<sup>a</sup>

<sup>a</sup> Department of Medicinal Chemistry, Amgen Inc., One Kendall Square, Bldg. 1000, Cambridge, MA 02139, USA

<sup>b</sup> Department of Molecular Structure, Amgen Inc., One Kendall Square, Bldg. 1000, Cambridge, MA 02139, USA

<sup>c</sup> Department of Pharmaceuticals, Amgen Inc., One Kendall Square, Bldg. 1000, Cambridge, MA 02139, USA

<sup>d</sup> Department of Pharmacokinetics and Drug Metabolism, Amgen Inc., One Kendall Square, Bldg. 1000, Cambridge, MA 02139, USA

<sup>e</sup> Department of Oncology Research, Amgen Inc., One Amgen Center Drive, Thousand Oaks, CA 91320, USA

<sup>f</sup> Department of Molecular Structure, Amgen Inc., One Amgen Center Drive, Thousand Oaks, CA 91320, USA

<sup>g</sup> Department of Pharmacokinetics and Drug Metabolism, Amgen Inc., One Amgen Center Drive, Thousand Oaks, CA 91320, USA

## ARTICLE INFO

## Article history:

Received 30 August 2008

Revised 12 November 2008

Accepted 17 November 2008

Available online 20 November 2008

## Keywords:

Tie-2 kinase  
Angiogenesis  
Kinase inhibitor  
Benzimidazole

## ABSTRACT

Selective small molecule inhibitors of Tie-2 kinase are important tools for the validation of Tie-2 signaling in pathological angiogenesis. Reported herein is the optimization of a nonselective scaffold into a potent and highly selective inhibitor of Tie-2 kinase.

© 2008 Elsevier Ltd. All rights reserved.

Receptor tyrosine kinases expressed by vascular endothelial cells are emerging as important mediators of pathological angiogenesis.<sup>1</sup> It is well established that activation of KDR (VEGFR2) by vascular endothelial growth factor (VEGF) strongly promotes angiogenesis by enhancing endothelial cell proliferation and survival.<sup>2</sup> In contrast, the precise role of the Tie-2 receptor in pathological angiogenesis has been difficult to ascertain, due to the existence of numerous endogenous ligands, including Angiopoietin-1 (Ang-1) and Angiopoietin-2 (Ang-2), which exhibit context-dependent activities.<sup>3</sup> We hypothesized that a small molecule Tie-2 kinase inhibitor with selectivity over KDR could be used to clarify the role of Tie-2 signaling in pathological angiogenesis.<sup>4</sup> Reported herein is the optimization of a nonselective scaffold into a potent, highly selective (>2500-fold over KDR), and orally available inhibitor of Tie-2 kinase.

Structural modification of an existing kinase inhibitor series<sup>4c</sup> provided a pyridyl-pyrimidine urea derivative **1** that is a potent,

nonselective inhibitor of Tie-2 and KDR (Fig. 1). Further modification involving replacement of the *N,N'*-diaryurea with *N*-arylbenzimidazole gave analog **2**. This molecule exhibited significantly weaker inhibition of Tie-2 as well as KDR. To our surprise, compound **4**, which lacks the lipophilic trifluoromethyl group, proved to be a reasonably potent and highly selective Tie-2 inhibitor. This finding was not expected based on the diminished potency and

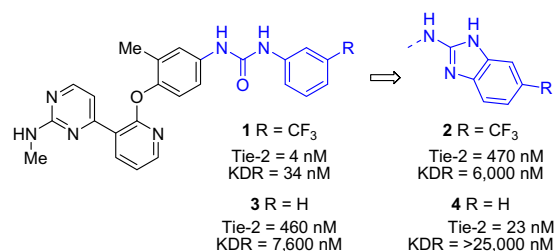


Figure 1. Discovery of a potent and selective Tie-2 inhibitor.

\* Corresponding author. Tel.: +1 805 313 5500; fax: +1 805 480 1337.

E-mail address: [vcee@amgen.com](mailto:vcee@amgen.com) (V.J. Cee).

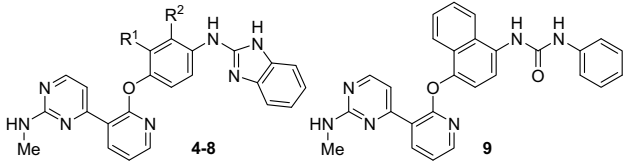
selectivity of analogous urea **3**. Given the promising selectivity of **4**, an effort was initiated to further optimize this series.

X-ray co-crystal structures of related phenoxy-substituted pyridyl pyrimidines bound to the Tie-2 kinase domain indicate that the aminopyrimidine engages in a series of hydrogen bonds with the hinge region of the kinase, with the central *para*-aminophenoxy ring occupying a hydrophobic pocket.<sup>4c</sup> Modifications to the central ring were undertaken with the goal of improving Tie-2 potency (Table 1). The initial monomethyl-substituted analog **4** has an IC<sub>50</sub> of 23 nM, with a 10-fold higher IC<sub>50</sub> of 250 nM for inhibition of Ang-1-stimulated Tie-2 phosphorylation in the Ea.hy926 endothelial cell line. The desmethyl analog (**5**), regioisomer (**6**), and dimethyl analog (**7**) all exhibit 10- to 20-fold reduced potency for Tie-2 inhibition. Ultimately, naphthalene was found to be the ideal central ring, with **8** exhibiting IC<sub>50</sub> values of 1 nM for Tie-2 enzyme and 20 nM for Tie-2 autophosphorylation in cells. Weak but measurable inhibition of KDR is evident for compound **8** (1400 nM), but the selectivity is still 1400-fold in favor of Tie-2. The importance of the benzimidazole appendage in achieving selectivity against KDR is evident from the corresponding urea **9**, which exhibits only 8-fold selectivity.

With the optimal central ring identified, our attention turned to modification of the aminobenzimidazole portion of molecule **8** (Table 2). Lipophilic substituents (Me, CF<sub>3</sub>) as the R<sup>1</sup> and R<sup>2</sup> groups, respectively, reduce Tie-2 potency, with the trifluoromethyl-substituted **11** exhibiting a striking increase in potency for inhibition of KDR, resulting in a relatively nonselective dual inhibitor. Methylation or replacement of the benzimidazole ring N–H results in reduced potency for inhibition of Tie-2, but significantly enhanced inhibition of KDR (**12–14**).

Compound **8** emerged as a very potent inhibitor of Tie-2 with excellent selectivity against KDR (1400×), and as such appeared to be an ideal molecular tool for further studies of Tie-2 in pathological angiogenesis. Profiling against a panel of 20 tyrosine and serine/threonine kinases indicated generally good selectivity, with significant activity (IC<sub>50</sub> < 100 nM) for Aurora A/B and JNK kinases. The inhibitory activity of **8** toward the purified Aurora kinase enzymes was confirmed in a cell-based assay: **8** induced aborted cytokinesis and ≥4 N DNA content in HeLa cells with an EC<sub>50</sub> of 120 nM.<sup>5</sup> Lack of meaningful Aurora kinase selectivity raised a potential concern as the Aurora kinases are important in the function of normal cell division.<sup>6</sup> As the impact of JNK inhibition on angio-

**Table 1**  
SAR of the central aryl ring (4–9)



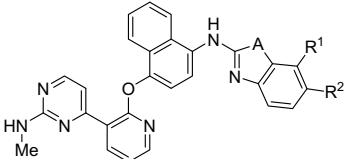
Compound	R <sup>1</sup>	R <sup>2</sup>	Enzyme IC <sub>50</sub> <sup>a</sup> (nM)		Cellular IC <sub>50</sub> <sup>b</sup> (nM)
			Tie-2	KDR	Tie-2 (Ea.hy926)
<b>4</b>	Me	H	23 ± 4	>25,000	250 ± 70
<b>5</b>	H	H	250 ± 30	>25,000	ND
<b>6</b>	H	Me	590 ± 70	>25,000	ND
<b>7</b>	Me	Me	310 ± 30	>25,000	ND
<b>8</b>	–(CH) <sub>4</sub> –		1 ± 0.6	1400 ± 90	20 <sup>c</sup>
<b>9</b>			5 ± 0.1	40 ± 14	ND

<sup>a</sup> Values are means of two to four experiments. Kinase assays run at the K<sub>m</sub> for ATP with final [ATP] of 5 μM for Tie-2 and 1 μM for KDR.

<sup>b</sup> Inhibition of Ang-1 stimulated Tie-2 phosphorylation in Ea.hy926 cells. ND, not determined.

<sup>c</sup> One experiment.

**Table 2**  
SAR of the aminobenzimidazole region



Compound	A	R <sup>1</sup>	R <sup>2</sup>	Enzyme IC <sub>50</sub> <sup>a</sup> (nM)	
				Tie-2	KDR
<b>8</b>	NH	H	H	1 ± 0.6	1400 ± 90
<b>10</b>	NH	Me	H	110 ± 14	1570 ± 170
<b>11</b>	NH	H	CF <sub>3</sub>	27 ± 6	69 ± 10
<b>12</b>	NMe	H	H	240 ± 170	250 ± 3
<b>13</b>	O	H	H	16 ± 2	30 ± 0.2
<b>14</b>	S	H	H	44 ± 4	88 ± 5

<sup>a</sup> Values are means of two to four experiments. Kinase assays run at the K<sub>m</sub> for ATP with final [ATP] of 5 μM for Tie-2 and 1 μM for KDR.

genesis is not well understood from the literature, this off-target activity was not addressed.<sup>7</sup>

The strategy for reducing inhibition of the Aurora kinases was guided by an X-ray co-crystal structure of urea **1** bound to Aurora A (Fig. 2).<sup>8</sup> Unlike previously obtained co-crystal structures of 4-(2-phenoxy-pyridin-3-yl)pyrimidines and Tie-2, the lipophilic methyl substituent of the central aryl ring does not occupy the hydrophobic pocket. This finding suggests that the hydrophobic pocket of the Aurora kinases is limited in size relative to Tie-2.

We reasoned that methyl-substituted analog **15** (Table 3) would not be accommodated by the Aurora kinases due to the presence of two substituents *ortho* to the phenoxy linkage. Relative to the parent compound **8**, compound **15** retains excellent potency for Tie-2 enzyme inhibition (IC<sub>50</sub> = 2 nM), high selectivity against KDR (>2500×), and exhibits better potency for inhibition of Tie-2 autophosphorylation in Ea.hy926 cells (IC<sub>50</sub> = 2 nM). Confirming our hypothesis, **15** exhibits approximately 2- and 8-fold less inhibitory activity for Aurora A and B enzymes, respectively, and most importantly, **15** does not induce phenotypic changes at concentrations up to 1.2 μM in a cell-based assay. Therefore, compound **15** possesses excellent cellular selectivity (>600×) against the Aurora kinases. This structural change did not, however, reduce the ability of **15** to inhibit the JNK family of kinases.

The synthesis of **15** (Scheme 1) is representative of the 4-(2-phenoxy-pyridin-3-yl)pyrimidines **4–15**. Coupling of 4-amino-2-methylnaphthalen-1-ol and the previously reported 4-(2-chloropyridin-3-yl)-*N*-methylpyrimidin-2-amine **16**<sup>4c</sup> occurred readily in the presence of cesium carbonate at high temperature. Conversion of the aniline into the corresponding isothiocyanate was accomplished with di-2-pyridyl thionocarbonate.<sup>9</sup> Polymer-supported carbodiimide, a convenient desulfurizing agent,<sup>10</sup> facilitated

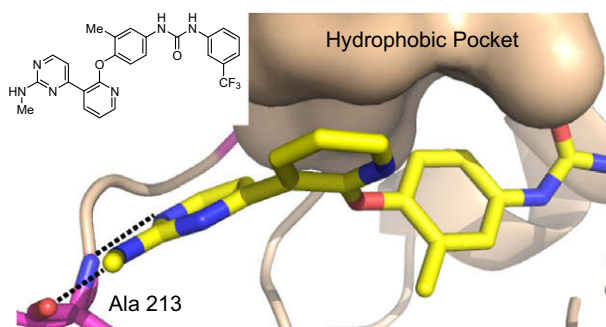
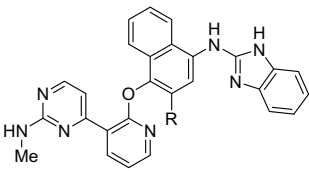


**Figure 2.** X-ray co-crystal structure of Aurora A and urea **1**.

**Table 3**  
Elimination of cellular Aurora activity



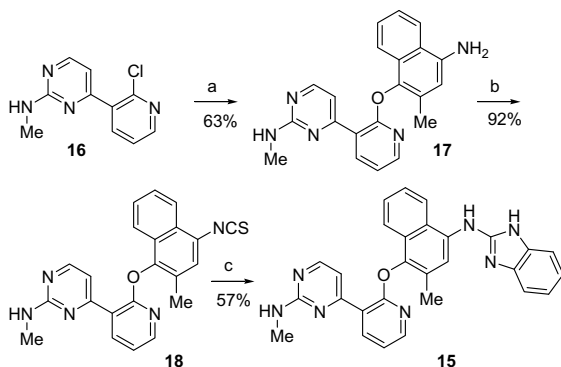
Compound	R	Enzyme IC <sub>50</sub> <sup>a</sup> (nM)			Cellular IC <sub>50</sub> (nM)	
		Tie-2	KDR	Aur A/B	Tie-2 <sup>b</sup>	Aurora <sup>c</sup>
<b>8</b>	H	1 ± 0.6	1400 ± 90	19 ± 11/10 ± 2	20 <sup>d</sup>	120 <sup>d</sup>
<b>15</b>	Me	2 ± 0.7	>5000	28 ± 1/80 ± 50	2 ± 0.4	>1200 <sup>d</sup>

<sup>a</sup> Values are means of two to four experiments. Kinase assays run at the  $K_m$  for ATP with final [ATP] of 5  $\mu$ M for Tie-2, 1  $\mu$ M for KDR, 8.2  $\mu$ M for Aurora A and 23  $\mu$ M for Aurora B.

<sup>b</sup> Inhibition of Ang-1 stimulated Tie-2 phosphorylation in Ea.hy926 cells.

<sup>c</sup> EC<sub>50</sub> for induction of  $\geq 4$ N phenotype by cellular imaging in HeLa cells.

<sup>d</sup> One experiment.



**Scheme 1.** Synthesis of **15**. Reagents and conditions: (a) 4-amino-2-methylnaphthalen-1-ol, Cs<sub>2</sub>CO<sub>3</sub>, DMSO, 130 °C; (b) di-2-pyridyl thionocarbonate, CH<sub>2</sub>Cl<sub>2</sub>; (c) 1,2-phenylene diamine, PS-carbodiimide, THF, 70 °C.

the condensation of **18** and 1,2-phenylenediamine to give aminobenzimidazole **15**.

While it was not possible to obtain a structure of **15** bound to Tie-2, an X-ray co-crystal structure was obtained for **15** bound to JNK3 (Fig. 3A). The molecule occupies the ATP binding pocket, with the aminopyrimidine within hydrogen-bonding distance of the hinge residue Met149. The central naphthalene ring projects into the hydrophobic pocket. The aminobenzimidazole is positioned to hydrogen bond with the backbone C=O of the activation loop residue Leu206 and the side chain of Lys93. The terminal phenyl portion of the benzimidazole occupies a relatively hydrophobic groove bounded on one side by the  $\alpha$ -C-helix and by leucine side chains from the N-terminal kinase domain on the other.

A homology model of Tie-2/**15** was constructed based on the JNK3/**15** structure (Fig. 3B).<sup>11</sup> The major residue differences between JNK3 and Tie-2 are Met146 to Ile902 'gatekeeper residue', Ala108 to Phe869 and Leu95 to Met857. These differences do not appear to significantly hinder binding of **15** to Tie-2. The position of the benzimidazole ring in the Tie-2/**15** homology model is remarkably similar to the inhibitory position observed for Phe983 in the reported Tie-2 apo crystal structure (Fig. 3C).<sup>12</sup> Apparently, KDR cannot adopt this binding mode or is much less accommodating of **15** in this binding mode.

The inability of KDR to accommodate compound **15** led us to speculate that the nonselective dual inhibitors **11–14** bind to KDR in a significantly different conformation. The structure of **11** (KDR IC<sub>50</sub> = 69 nM) bound to KDR was obtained (Fig. 3D). The ami-

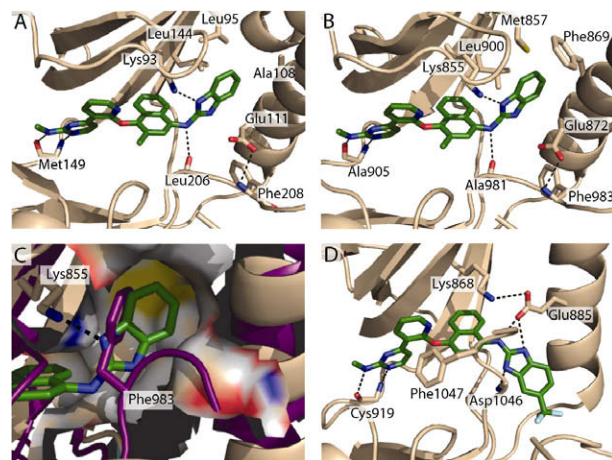


**Figure 3.** (A) X-ray co-crystal structure of **15** bound to JNK3. (B) Homology model of **15** bound to Tie-2. (C) Overlay of Tie-2 apo (purple) and bound (wheat) with surface rendering of benzimidazole binding pocket. (D) X-ray co-crystal structure of **11** bound to KDR.

nobenzimidazole occupies a strikingly different position, with hydrogen-bonding interactions with  $\alpha$ -C-helix residue Glu885 and the backbone N–H of activation loop residue Asp1046. The activation loop is positioned in the inactive DFG-out conformation,<sup>13</sup> with the lipophilic trifluoromethyl-arene portion of the benzimidazole occupying the extended hydrophobic pocket. Presumably, the absence of the lipophilic trifluoromethyl group in compounds **8** and **15** results in suboptimal interactions in the extended hydrophobic pocket, leading to poor binding to KDR.

Comparison of the bound structure of the KDR-selective Tie-2 inhibitor **15** derived from the JNK3/**15** co-crystal with the bound structure of the KDR-selective Tie-2 inhibitor **19** derived from a previously reported Tie-2/**19** co-crystal<sup>4c</sup> reveals that the benzimidazole ring of **15** and the morpholine ring of **19** occupy similar space (Fig. 4). As structure–activity relationships have demonstrated that the benzimidazole of **15** and morpholine of **19** are key to achieving selectivity for Tie-2 over KDR, both molecules appear to benefit by occupying the hydrophobic pocket of Tie-2 identified in Figure 3C.

Compound **15** possessed acceptable pharmacokinetic properties in rat (Table 4) characterized by a moderate clearance (Cl) and large volume of distribution ( $V_{ss}$ ) which resulted in a relatively long half life of 3.7 h. When orally dosed as a suspension to rats, the bioavailability was 26%.

The ability of **15** to modulate Tie-2 phosphorylation levels in vivo was assessed in a mouse pharmacodynamic model, in which Tie-2 phosphorylation in mouse lung tissue is stimulated by human Angiopoietin-1 (h-Ang-1) (Fig. 5).<sup>4c</sup> A dose-dependent inhibition of stimulated Tie-2 phosphorylation was observed, with Tie-2 phosphorylation reduced to sub-basal levels with a single oral dose of  $\geq 30$  mg/kg. The 10 mg/kg dose provided an approximately 50% reduction in stimulated Tie-2 phosphorylation, with a plasma concentration of 260 nM **15**. This concentration is 130-

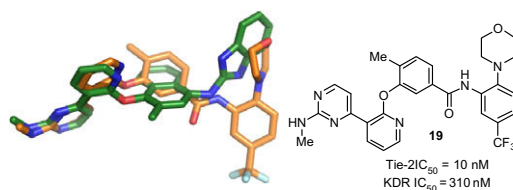


**Figure 4.** Overlay of selective Tie-2 inhibitors **15** (green) and **19** (orange) from X-ray co-crystal structures with JNK3 and Tie-2, respectively.

**Table 4**  
Pharmacokinetic properties of **15** in male Sprague–Dawley rats

Cl (mL/min/kg) <sup>a</sup>	V <sub>ss</sub> (mL/kg) <sup>a</sup>	T <sub>1/2</sub> (h) <sup>a</sup>	F (%) <sup>b</sup>
28	5900	3.7	26

<sup>a</sup> iv, 0.5 mg/kg, DMSO.

<sup>b</sup> po, 5 mpk, OraPlus pH = 2.

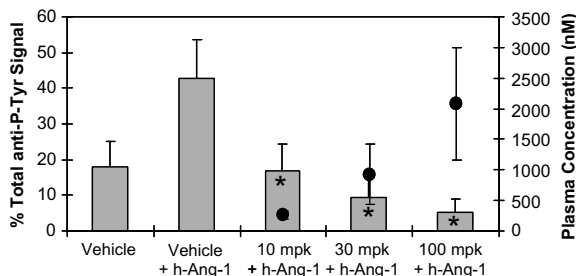


**Figure 5.** Compound **15** inhibits h-Ang-1 stimulated Tie-2 phosphorylation in mouse lung. Data points represent the mean  $\pm$  SD,  $n = 3$ ; (\*)  $p \leq 0.05$  versus vehicle + h-Ang-1 by one-way ANOVA with Dunnett's post-hoc test. Bars represent phosphorylated Tie-2, and circles represent plasma concentration of **15**.

fold greater than the cellular IC<sub>50</sub> of **15** (2 nM). However, taking into account nonspecific binding to mouse plasma proteins (**15** = 99.6% bound in mouse plasma), the free unbound fraction of **15** is 1 nM, approximately equivalent to the IC<sub>50</sub> determined in the cell-based assay (2 nM). The robust inhibition of Tie-2 phosphorylation upon oral administration of **15** indicates that this molecule may be a suitable tool for the in vivo evaluation of Tie-2 signaling in angiogenesis.

**Conclusion:** An effort to reduce KDR inhibitory activity of the dual Tie-2/KDR inhibitor **1** resulted in **15**, a potent Tie-2 inhibitor (IC<sub>50</sub> = 2 nM) with excellent selectivity over KDR (>2500 $\times$ ) and selectivity in cell-based assays over Aurora (>600 $\times$ ). Structural information from a JNK3/**15** co-crystal suggests a DFG-in binding mode in Tie-2 that is not tolerated by KDR. In a mouse pharmacodynamic model, **15** exhibited a dose-dependent inhibition of Ang-1-stimulated Tie-2 phosphorylation in lung tissue, indicating that

**15** may be a suitable tool for the in vivo evaluation of Tie-2 signaling in angiogenesis.

## Acknowledgments

We thank Melanie Cooke for formulation support, Bethlyn Jaramilla for bioanalytical support, Shane Johnson for plasma protein binding, Marc Payton and Patrick Eden for the HeLa cell assay, and Jin Tang for purification of Aurora A/B proteins.

## References and notes

- (a) Folkman, J. *Nat. Rev. Drug Disc.* **2007**, *6*, 273; (b) Shawver, L. K.; Lipson, K. E.; Fong, T. A. T.; McMahon, G.; Plowman, G. D.; Strawn, L. M. *Drug Discovery Today* **1997**, *2*, 50; (c) Folkman, J. *Nat. Med.* **1995**, *1*, 27.
- Ferrara, N.; Gerber, H.-P.; LeCouter, J. *Nat. Med.* **2003**, *9*, 669.
- (a) Kim, K. L.; Shin, I.-S.; Kim, J.-M.; Choi, J.-H.; Byun, J.; Jeon, E.-S.; Suh, W.; Kim, D.-K. *Cardiovasc. Res.* **2006**, *72*, 394; (b) Yu, Q. *Future Med.* **2005**, *1*, 475; (c) Peters, K. G.; Kontos, C. D.; Lin, P. C.; Wong, A. L.; Rao, P.; Huang, L.; Dewhirst, M. W.; Sankar, S. *Recent Prog. Horm. Res.* **2004**, *59*, 51; (d) Jones, N.; Iljin, K.; Dumont, D. J.; Alitalo, K. *Nat. Rev. Mol. Cell Biol.* **2001**, *2*, 257.
- (a) Johnson, N. W.; Semones, M.; Adams, J. L.; Hansbury, M.; Winkler, J. *Bioorg. Med. Chem. Lett.* **2007**, *17*, 5514; (b) Cee, V. J.; Albrecht, B. K.; Geuns-Meyer, S. D.; Hughes, P. E.; Bellon, S.; Bready, J.; Caenepeel, S.; Chaffee, S. C.; Coxon, A.; Emery, M.; Fretland, J.; Gallant, P.; Gu, Y.; Hodous, B. L.; Hoffman, D.; Johnson, R. E.; Kendall, R.; Kim, J. L.; Long, A. M.; McGowan, D.; Morrison, M.; Olivieri, P. R.; Patel, V. F.; Polverino, A.; Powers, D.; Rose, P.; Wang, L.; Zhao, H. *J. Med. Chem.* **2007**, *50*, 627; (c) Hodous, B. L.; Geuns-Meyer, S. D.; Hughes, P. E.; Albrecht, B. K.; Bellon, S.; Bready, J.; Caenepeel, S.; Cee, V. J.; Chaffee, S. C.; Coxon, A.; Emery, M.; Fretland, J.; Gallant, P.; Gu, Y.; Hoffman, D.; Johnson, R. E.; Kendall, R.; Kim, J. L.; Long, A. M.; Morrison, M.; Olivieri, P. R.; Patel, V. F.; Polverino, A.; Rose, P.; Tempest, P.; Wang, L.; Whittington, D.; Zhao, H. *J. Med. Chem.* **2007**, *50*, 611, and references therein.
- Polyploidy is a hallmark of Aurora B or Aurora A/B inhibition: Yang, H.; Burke, T.; Dempsey, J.; Diaz, B.; Collins, E.; Toth, J.; Beckmann, R.; Ye, X. *FEBS Lett.* **2005**, *579*, 3385.
- Carmena, M.; Earnshaw, W. C. *Nat. Rev. Mol. Cell Biol.* **2003**, *4*, 842.
- The JNK inhibitor SP600125 is reported to impact tumor growth and angiogenesis, but this is likely an off-target activity: Schmidt, M.; Budirahardja, Y.; Klompaker, R.; Medema, R. *EMBO Rep.* **2005**, *6*, 866.
- Atomic coordinates for the Aurora A/1, JNK3/15, and KDR/11 crystal structures have PDB Codes 3EFW, 3DA6, and 3EWH, respectively.
- Kim, S.; Yi, K. Y. *Tetrahedron Lett.* **1985**, *26*, 1661.
- Cee, V. J.; Downing, N. S. *Tetrahedron Lett.* **2006**, *47*, 3747.
- SCWRL 3.0 was used for initial side-chain rotamer replacement using the Tie-2 sequence, and the resulting model underwent restrained energy minimization using the AMBER89 force-field implemented in MOE 2006.08 (Chemical Computing Group, Montreal, Canada).
- Shewchuk, L. M.; Hassell, A. M.; Ellis, B.; Holmes, W. D.; Davis, R.; Horne, E. L.; Kadwell, S. H.; McKee, D. D.; Moore, J. T. *Structure* **2000**, *8*, 1105.
- Cherry, M.; Williams, D. H. *Curr. Med. Chem.* **2004**, *11*, 663.